

## NUMERICAL SIMULATION OF THE NOZZLE AND EJECTOR EFFECT ON THE PERFORMANCE OF A PULSE DETONATION ENGINE

by

**Zhiwu WANG<sup>a\*</sup>, Xing LIU<sup>a</sup>, Yaqi WANG<sup>a</sup>, Hongwei LI<sup>a</sup>,  
Kun ZHANG<sup>b</sup>, and Longxi ZHENG<sup>a</sup>**

<sup>a</sup>School of Power and Energy, Northwestern Polytechnical University, Xi'an, China

<sup>b</sup>Avic Xi'an Aero-Engine (group) Ltd., Xi'an, China

Original scientific paper

<https://doi.org/10.2298/TSCI170319294W>

*Single-shot pulse detonation engine (PDE) with three different types of nozzles-straight ejector combinational structures at three different ejector positions were simulated by the unsteady 2-D axisymmetric method. Three types of nozzles included the straight nozzle, convergent nozzle and convergent-divergent nozzle. Propane was used as the fuel and air as the oxidizer. The simulation results indicated that the PDE with a straight nozzle and PDE with a convergent-divergent nozzle obtained improved performance when an ejector was added at all of the three ejector positions ( $x/d = -1, 0$  and  $+1$ ), and PDE with a convergent-divergent nozzle gained the larger improved performance at all the three ejector positions. The PDE with a convergent nozzle-ejector combinational structure obtained the slightly worse performance at the ejector position of  $x/d = -1$ , gained the slightly increased performance at the ejector position of  $x/d = 0$ , and achieved the largest impulse augmentation and the second largest ejection ratio at the ejector position of  $x/d = +1$  among all of the nine cases of the nozzle-ejector combinational structures. Ejector position of  $x/d = +1$  was the best ejection position at which the PDE with a convergent nozzle-ejector combinational structure achieved the best propulsion performance, ejector position of  $x/d = -1$  was the best ejector position for the PDE with a convergent-divergent nozzle-ejector combinational structure, and ejector position of  $x/d = 0$  was the best ejector position for the PDE with a straight nozzle-ejector combinational structure.*

Key words: *ejector; nozzle, numerical simulation, performance*

### Introduction

A PDE is a kind of unsteady propulsion system that generates the thrust based on the high temperature and high pressure products resulted from pulsed detonation [1-3]. Compared with other conventional propulsion systems, a PDE has two notable characteristics: unsteady operation and detonation combustion process. Fundamental and applied PDE research has been carried out over the last several decades around the world because of its potential advantages of high thermal cycle efficiency, simple construction, wide operating range and low specific fuel consumption [4-6]. Thrust or impulse is an important index to measure the propulsive performance of a PDE. One of the ways to improve the PDE specific impulse is installing an ejector at the engine outlet to eject fresh air [7-10].

\* Corresponding author, e-mail: malsoo@mail.nwpu.edu.cn

Wilson *et al.* [11] proposed a fast and efficient performance evaluation method for the PDE-ejector, which combined the performance parameters calculation method of an ideal PDE by Endo Fujiwawa with the improved Heiser Pratt steady-state ejector model. Glaser *et al.* [12] found that the ejector performance was deeply related with the axial distance between the ejector inlet and the detonation tube outlet. The thrust augmentation was reduced when the ejector was located at the upstream of the detonation tube. However, this conclusion was not consistent with that of Bravo [13]. Choutapalli *et al.* [14] found that the initial vortex caused by the jet from the nozzle would induce a new secondary vortex at the wall surface of the ejector and the eddy flux was the largest when the thrust augmentation gained the maximum value. Meanwhile, they also concluded that the mixing performance was improved and the thrust was increased by the anticlockwise vortex in the ejector tube. Opalski [15] found that the ratio of the vortex ring to the ejector diameter had a great influence on the PDE thrust augmentation. Kazuhiko *et al.* [16] designed a supersonic nozzle ejector to increase the thrust of single pulse detonation for methane-oxygen and hydrogen-oxygen mixtures based on the conventional characteristic method. Farahi *et al.* [17] presented a new method for designing a nozzle. Peng *et al.* [18] conducted an experiment to improve the performance of ejector driven by an air-breathing PDE with a convergent nozzle. He *et al.* [19, 20] carried out the numerical simulation on PDE-ejector performance, which showed that only the convergent-divergent (CD) ejector gained a positive thrust augmentation for the PDE. The impulse augmentation (IA) increased but the ejector secondary flow rate decreased at the decreased ejector throat area. In order to solve the ground startup problems of a pulse PDE, Li *et al.* [21] numerically simulated the multi-cycle rocket-ejector mode of a pulse detonation rocket engine (namely the ejecting process of a detonation tube with a straight ejector) by the unsteady 2-D axisymmetric method. Qin *et al.* [22] obtained the parameters distribution of a detonation wave in the detonation tube by analytical method and numerically simulated the propagation and exhaust processes after a detonation wave was degenerated to a shock wave. Huang *et al.* [23] researched the thrust of PDE with ejector by experiments and found that the ejector can improve the thrust of PDE evidently, while the highest augmentation was obtained when the ejector was equipped at downstream of the nozzle. Wang *et al.* [24] designed a model of PDE, the engine was operated at 5-8 Hz successfully and found that the PDE with ejector mode had shorter deflagration to detonation transition (DDT) distance compared to the conventional situation. Guo *et al.* [25] simulated the exhaust process of 2-D divergent ejector by detailed chemistry mechanism method. The results showed that the divergent ejector can improve the integral impulse of single cycle 12.5%.

There are many factors that affected the performance of the PDE transient ejector. Some researchers had done a lot of research on the PDE transient ejector, but the conclusion was different and even contradictory. Up to now, the combination effect of the nozzle type and ejector position on the PDE performance has not been studied systematically. This paper focuses on the numerical studied of the ejector position effect on the propulsive performance of the PDE based on the combinational structures consisted of three different types of nozzles and a straight ejector. Three types of nozzles included the straight nozzle, convergent nozzle and convergent-divergent (CD) nozzle. Some useful results were obtained and provided the reference to the optimal design of the PDE nozzle and ejector.

### Physical models

Three parts were included in the computational domain, a detonation tube, an ejector and the external region. The left end of the detonation tube was closed as the thrust wall, while the right end was open for exhausting. There are two key geometry requirements to initiate a

detonation in the detonation tube,  $d \geq \lambda/\pi$  and  $L \geq L_{DDT}$ , where,  $d$  represents the inner diameter of the detonation tube,  $\lambda$  represents the fuel cell size,  $L$  and  $L_{DDT}$  represent the length of the detonation tube and the DDT distance, respectively. For gas phase detonation, distance of DDT is generally in the range of ten times of  $\lambda$ . In this paper,  $L$  was 902 mm and  $d$  was 30 mm. The ignition zone with the width of 2 mm was close to the left end. The length of the nozzles was constant, 40 mm.

This paper mainly studied the ejecting performance based on three types of nozzle and ejector combinational structures at different axial positions. The convergent angle of the convergent nozzle was  $9^\circ$ . The convergent and divergent angles of the CD nozzle were both  $5^\circ$ . The ejector was a straight ejector with the inner diameter of 82 mm. Nine nozzle-ejector combinational models are shown in fig. 1. The external region of  $900 \text{ mm} \times 400 \text{ mm}$  was used to simulate the outlet boundary of the detonation tube. The length of axial overlapping section between the external region and the detonation tube was 240 mm. Structured quadrilateral mesh was adopted as the computational grid. The external region of the domain is pressure outlet. According to the research of Wang *et al.* [26], the result of detonation initiation and hot jet was independent with the size of the mesh, so in order to obtain the accurate result by efficiently calculation, the grid size of the detonation tube was chosen as 0.5 mm, and the grid size of the left computational area was chosen as 1 mm. The total points of the meshes was about 0.1 million. The adaptive mesh was used to achieve the goal of grid-independence.

In this paper, the benchmark cases without an ejector but a straight nozzle, convergent nozzle, and CD nozzle were represented by Case 1, Case 2, and Case 3, respectively. Case 4, Case 5, and Case 6, represented the cases in which the PDE equipped with the straight nozzle-ejector at three different ejector positions of  $x/d = -1, 0, +1$ , where  $x$  represented the distance between the nozzle outlet and the ejector inlet. Similarly, Case 7, Case 8, and Case 9, represented the cases where the PDE equipped with the convergent nozzle-ejector at the three different ejector positions. Case 10, Case 11, and Case 12, denoted the cases where the PDE equipped with the CD nozzle-ejector at the three different ejector positions.

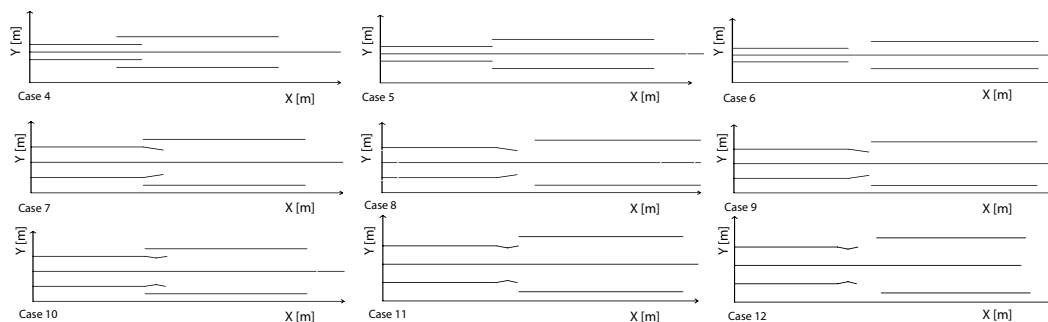


**Figure 1. Simulation models for the different nozzle and ejector combinational structures**

Unsteady axisymmetric 2-D simulations were performed by solving the compressible Navier-Stokes equations with the finite volume method. A single-step irreversible finite rate chemical kinetic model was adopted in the present work to consider the effect of the source term created by the chemical reactions. The standard  $k-\epsilon$  turbulence model was employed in all the simulations. Standard wall function method was used to deal with the flow near the tube wall. The PISO scheme was used in the situation and the method of discrete of the transient formulation was second order implicit scheme. The adaptive mesh refinement method was used

to refine the local mesh where there were large pressure gradients. The gas was assumed as an ideal gas, and the transport processes were ignored. Stoichiometric propane/air mixture was used as the combustible mixture in the detonation tube. The initial temperature was 300 K and the initial pressure was 0.1 MPa. The initial pressure and temperature of the ignition zone was 3 MPa and 1500 K.

**Table 1. Simulation results in the 12 cases and the CJ gaseous detonation wave parameters by CEA**

	$V$ [ms <sup>-1</sup> ]	$T$ [K]	$P$ [MPa]
CEA	1804.8	2821.2	1.869
Case 1	1920.20	3420	3.61
Case 2	1926.40	3410	3.52
Case 3	1922.67	3410	3.52
Case 4	1930.09	3440	3.65
Case 5	1930.50	3370	3.25
Case 6	1930.92	3370	3.23
Case 7	1930.50	3400	3.71
Case 8	1930.50	3390	3.51
Case 9	1930.50	3320	3.19
Case 10	1930.50	3320	3.06
Case 11	1928.85	3480	3.70
Case 12	1930.92	3360	3.17

## Calculation results and analysis

### Detonation initiation analysis

A fully developed detonation wave was judged by measuring and analyzing the velocity, pressure and temperature in the detonation tube. Table 1 shows the simulation results in the 12 cases and the Chapman-Jouguet (CJ) gaseous detonation wave parameters for the stoichiometric propane/air mixture calculated by chemical equilibrium and applications (CEA) code developed by NASA Lewis Research Center. As can be seen, the wave velocities of the numerical simulations were in the range of 1920.2-1930.92 m/s, the temperatures behind the detonation waves were between 3320 K and 3480 K, while the detonation pressures were between 3.06 MPa-3.71 MPa. The velocity, temperature and pressure of a CJ gaseous detonation wave calculated by CEA were 1804.8 m/s, 2821.2 K, and 1.869 MPa, respectively. Compared with the CEA calculation values, the numerical calculation results were basically reasonable.

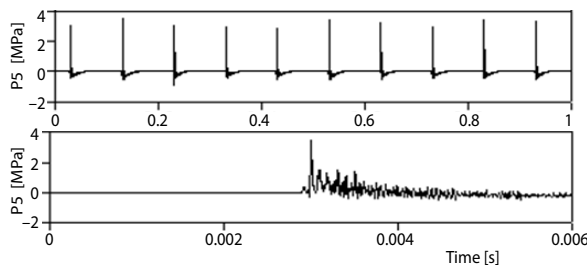


**Figure 2. The pressure history of PDE at 10 Hz and the enlarge graph of sixth cycle**

Figure 2 shows the pressure history of detonation in the detonation tube when the operating frequency is 10 Hz. The experiments was operated with the fuel of kerosene, which owns the similar properties with propane. The data of the pressure was collected by pressure sensor. As shown in the graph, the peak value of the pressure is nearly 3.5 MPa, which is very close to the value of the simulation. In this way, the results of the simulation are reliable.

### Transient thrust and impulse analysis

Figure 3 illustrates the instantaneous thrust curves and partial enlargements of Case 1, Case 4, Case 5, and Case 6. The thrust on the thrust platforms (thrust platforms is the range of time that the thrust not change with time) in the cases of Case 1, Case 4, and Case 5 were almost the same, while there was a transient high negative thrust peak value in Case 6. The thrust in all the four cases decreased during the exhaust process.

The instantaneous thrust curves and partial enlargements of Case 2, Case 7, Case 8, and Case 9 are shown in fig. 4. Because of the impact of the convergent nozzle, a negative thrust of about 1200 N occurred at  $t = 0.53$  ms followed by a positive thrust peak value and this phenomenon repeated for several times with the decreased peak values in Case 2, Case 7, and Case 8, while a positive thrust peak value appeared firstly at  $t = 0.4$  ms in Case 9 and then the variation trend of the instantaneous thrust was similar to that of the three cases. Each of the times that the shock waves from the convergent nozzle outlet collided with the ejector wall in the four cases was different due to the different ejector positions, so the back-propagation waves and the number of waves reflected from the thrust wall were different. Therefore, the times and the values of the positive and negative thrust peak were not the same. According to the partial enlargement of the instantaneous thrust curves in Case 2, Case 7, Case 8, and Case 9, the variation trends and values of the instantaneous thrust in Case 2, Case 7, and Case 8 were nearly the same while the thrust variation trends in Case 9 was similar to the previous three cases but the thrust values were much different especially after  $t = 1.5$  ms. Compared with Case 2, Case 7, and Case 8, the thrust peaks came ahead of time and the values were greater after the first thrust peak in Case 9.

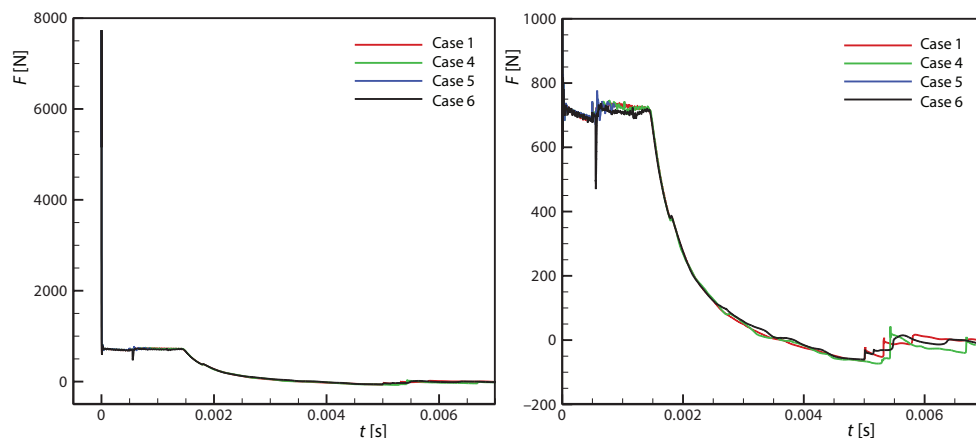


Figure 3. Instantaneous thrust curves and partial enlargement in Case 1 and Cases 4-6

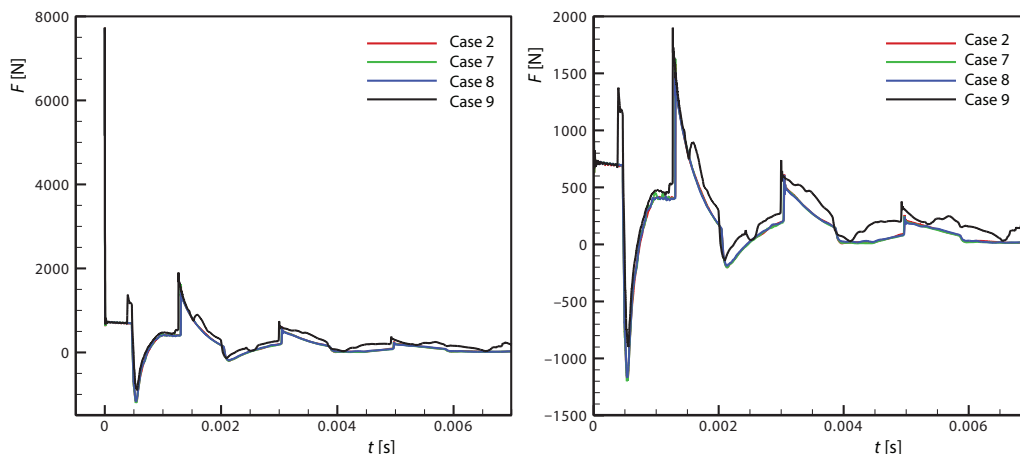


Figure 4. Instantaneous thrust curves and partial enlargement in Case 2 and Cases 7-9  
 (for color image see journal web site)

Figure 5 shows the instantaneous thrust curves and partial enlargements in Case 3, Case 10, Case 11, and Case 12. Because of the impact of the convergence-divergent nozzle, a sudden thrust drop occurred at the pressure plateau region, in which the amplitudes of the Case 10 and Case 12 were both the maximum, the amplitude in Case 11 was the minimum. After that, the thrust increased in all of the four cases and reached a period of platform area. Then the thrust increased suddenly and obtained a positive peak value. Similar to the sudden thrust drop, the increase amplitudes in Case 10 and Case 12 were both the maximum, the amplitude in Case 11 was the minimum.

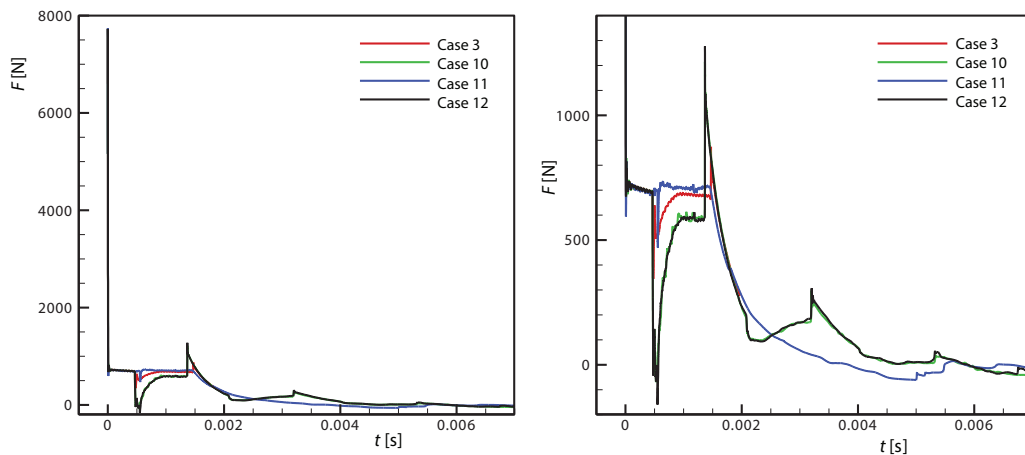


Figure 5. Instantaneous thrust curves and partial enlargement in Case 3 and Cases 10-12  
(for color image see journal web site)

Table 2 illustrates the propulsive performance of PDE with different types of nozzle-ejector combinational structures at different axial positions of ejector. The IA was defined as the ratio of the difference between the impulse of PDE with and without the ejector to the impulse of PDE without ejector. There were two types of IA. One was based on the data of the PDE with the corresponding nozzle without an ejector as shown in eq. (1), the other based on the data of the PDE with the straight nozzle without an ejector as shown in eq. (2).  $IA_{\text{straight}}$  represented the IA based on the straight nozzle (Case 1), while IA represented the impulse augmentation based on a convergent or CD nozzle (Case 2 or 3). The  $I$  represented the impulse of the PDE with a convergent or CD nozzle without ejector

Table 2. Impulse (N·s) and IA of PDE in 12 Cases

Nozzle type	Cases	Impulse	IA	$IA_{\text{straight}}$
Straight nozzle	Case 1	1.30853		
	Case 4	1.34608	2.87%	2.87%
	Case 5	1.4136	8.03%	8.03%
	Case 6	1.37833	5.33%	5.33%
Convergent nozzle	Case 2	1.31315		
	Case 7	1.29646	-1.27%	-0.92%
	Case 8	1.32024	0.54%	0.89%
	Case 9	2.09832	59.79%	60.36%
CD nozzle	Case 3	1.38093		
	Case 10	1.60298	16.08%	22.50%
	Case 11	1.39591	1.09%	6.68%
	Case 12	1.49042	7.93%	13.90%

(Case 2 or Case 3), while  $I_{\text{straight}}$  represented the impulse of the PDE with the straight nozzle without ejector (Case 1) and  $I_{\text{ejector}}$  represented the impulse of the PDE with a nozzle-ejector. For the PDE with the convergent nozzle, ejector had little influence on the performance of PDE at the ejector positions of  $x/d = -1$  and 0, which just gained  $-0.92\%$  and  $0.89\%$  IA. However, a larger IA was obtained at the ejector position of  $x/d = +1$ . For the PDE with the straight nozzle and convergence-divergent nozzle, some IA was gained by using the ejector at all of the three ejector positions, among which larger IA was achieved when the ejector was installed to the PDE with a convergence-divergent nozzle. In all of the calculation models, the PDE with the convergent nozzle and ejector combinational structure got the maximum IA  $60.36\%$  at the ejector position of  $x/d = +1$ .

$$IA = \frac{I_{\text{ejector}} - I}{I} 100\% \quad (1)$$

$$IA_{\text{straight}} = \frac{I_{\text{ejector}} - I_{\text{straight}}}{I_{\text{straight}}} 100\% \quad (2)$$

### Mass-flow analysis

Figure 6 illustrates the instantaneous mass-flow rate curves at the nozzle outlet, ejector inlet and outlet of the PDE when the straight nozzle-ejector combinational structure was used and the ejector was installed at the position of  $x/d = -1$  (Case 4). The detonation wave expelled from the nozzle and the mass-flow rate at the nozzle outlet reached the peak value of about  $3.355 \text{ kg/s}$  at  $t = 0.4970 \text{ ms}$ . Meanwhile, the detonation wave degenerated to a shock wave and continued to propagate to the ejector inlet. Then, the main shock wave arrived at the ejector at about  $t = 0.6237 \text{ ms}$  and made the ejector inlet choked, which resulted in the first negative peak value of the mass-flow at the ejector inlet,  $-1.77 \text{ kg/s}$ . Subsequently, the main shock wave arrived at the ejector outlet at about  $t = 1.073 \text{ ms}$  and the mass-flow rate of the ejector outlet obtained a peak value of  $5.561 \text{ kg/s}$ . At the same time, a negative pressure zone was formed at the ejector inlet and the fresh air was introduced quickly. The mass-flow rate at the ejector inlet became positive from  $t = 2.043 \text{ ms}$ . Because of a decrease in static pressure and viscous shear forces within the ejector, the ejector will entrain flow into the inlet. The mass-flow rate at the ejector inlet was  $0.64 \text{ kg/s}$  at  $t = 3.0 \text{ ms}$  and then maintained a relatively constant.

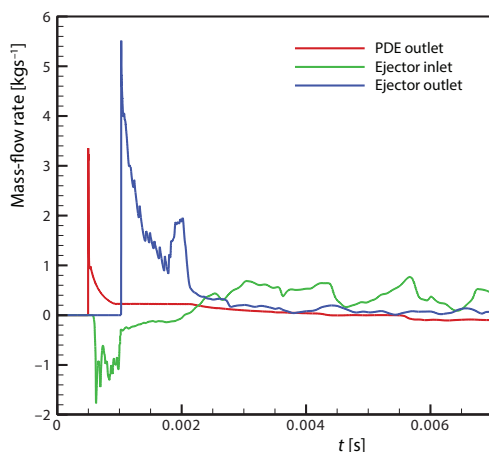


Figure 6. Mass-flow rate vs. time in Case 4  
 (for color image see journal web site)

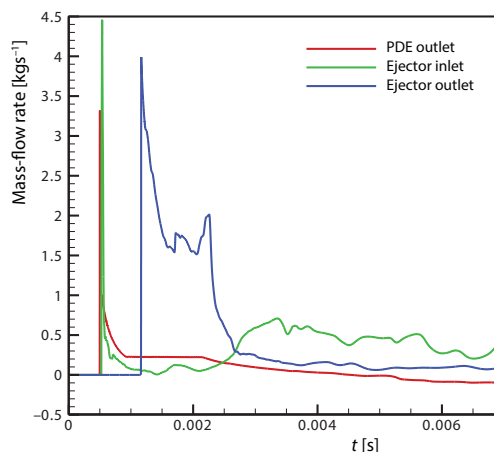


Figure 7. Mass-flow rate vs. time in Case 11  
 (for color image see journal web site)

The instantaneous mass-flow rate curves at the nozzle outlet, ejector inlet and outlet of the PDE with the CD nozzle-ejector combinational structure at the ejector position of  $x/d = 0$  (Case 11) are shown in fig. 7. The detonation wave expelled from the nozzle and the mass-flow rate at the nozzle outlet reached the peak value of about 3.3189 kg/s at  $t = 0.5013$  ms. The detonation wave degenerated to a shock wave and propagated to the inlet of the ejector. At about  $t = 0.5372$  ms, the main shock wave entered the ejector and the fresh air was introduced to the ejector, which was different from that of Case 4 due to the different nozzle type. Meanwhile, the mass-flow rate at the ejector inlet obtained the first positive peak value of about 4.4592 kg/s. After that, the mass-flow rate at the ejector inlet decreased sharply. The main shock wave arrived at the ejector outlet at about  $t = 1.166$  ms and the mass-flow rate at the ejector outlet gained the peak value of 3.989 kg/s. At the same time, a negative pressure zone was formed at the ejector inlet and the fresh air was introduced quickly, which led to the obvious increase of the mass-flow rate at the ejector inlet since  $t = 2.5$  ms. The mass-flow rate at the ejector inlet was 0.65 kg/s at  $t = 3.2$  ms and then maintained a relatively stable-state.

Figure 8 illustrates the instantaneous mass-flow rate curves at the nozzle outlet, ejector inlet and outlet of the PDE with the CD nozzle-ejector combinational structure at the ejector position of  $x/d = +1$  (Case 12). The detonation wave expelled from the nozzle and the mass-flow rate at the nozzle outlet reached the peak value of about 2.694 kg/s at  $t = 0.4956$  ms. The shock wave degenerated from a detonation wave spread to the ejector inlet. The mass-flow rate at the ejector inlet was equal to the sum of the mass-flow rate at the nozzle outlet and the mass-flow rate of fresh air ejected by the ejector. At about  $t = 0.534$  ms, the mass-flow rate at the ejector inlet gained the first peak value 3.9186 kg/s and was greater than the mass-flow rate at the nozzle outlet, which proved that the air near the ejector inlet was ejected to the ejector by entrainment when the main shock wave entered the ejector. A negative mass-flow rate peak value of  $-0.45497$  kg/s occurred at the ejector inlet at  $t = 0.696$  ms due to the influence of the convergent and divergent configuration of the nozzle. After that, the mass-flow rate at the ejector inlet increased and then maintained a relatively stable ejecting state since  $t = 3$  ms. The main shock wave arrived at the ejector outlet at about  $t = 1.183$  ms and the mass-flow rate at the ejector outlet gained the peak value of 3.701 kg/s.

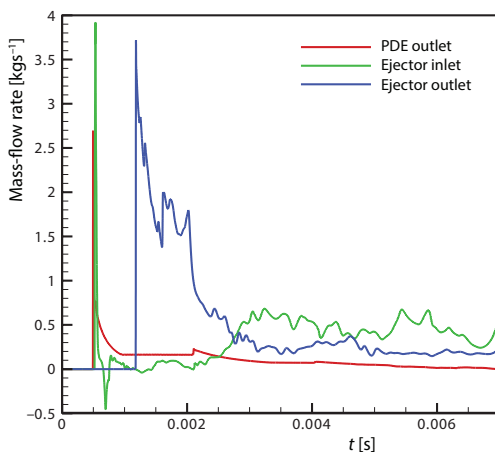


Figure 8. Mass-flow rate vs. time in Case 12  
 (for color image see journal web site)

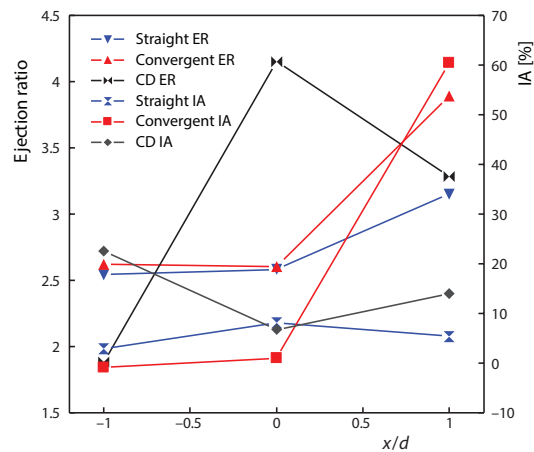


Figure 9. Ejection ratio and IA at different ejector positions

Figure 9 shows the relationship between the ejector ratio (ER), IA ratio ( $IA_{\text{straight}}$ ), and the ejector installation position for the PDE with three different types of nozzle-ejector combinational structures. The ER is the mass-flow rate of ejector divided the mass-flow rate of nozzle. The ER variation trend in the case of the straight nozzle was similar to that of the convergent nozzle. For the straight nozzle and the convergent nozzle, both of the two ER at the ejector position of  $x/d = -1$  and 0 were around 2.5, while the ER at the ejector position of  $x/d = +1$  increased significantly. The ER of the convergent nozzle at the ejector position of  $x/d = +1$  was larger than that of the straight nozzle. Big difference occurred at the different ejector positions for the ER of the CD nozzle, in which the largest ejection ratio of 4.15 was gained at the ejector position of  $x/d = 0$  but the lowest ER of only 1.88 at the ejector position of  $x/d = -1$ . It could be found that there was no certain relationship between the ER and the IA ratio. When the convergent nozzle-ejector combinational structure was used, the maximum IA and the second largest ER was obtained at the ejector position of  $x/d = +1$ . The maximum ER was gained with the CD nozzle-ejector combinational structure at the ejector position of  $x/d = 0$ , which was slightly greater than that of convergent nozzle-ejector at the ejector position of  $x/d = +1$ . As a whole, the best ejection performance was obtained based on the PDE with the convergent nozzle-ejector combinational structure at the ejector position of  $x/d = +1$ .

Figure 10 shows experiment results of the IA of the PDE with the operating frequency of 20 Hz. As shown in the graph, the trend of the augmentation of different combination is corresponding to the simulation result. The highest augmentation of straight IA appeared at position 0, while the convergent IA obtained the highest augmentation at position 1, the highest augmentation of the CD nozzle was observed at position -1. This trend is the same with the simulation while the value is some difference. This is caused by the operating frequency.

### Conclusions

In order to find the nozzle type and ejector combination effect on the PDE propulsion performance, three different types of nozzles including the straight nozzle, convergent nozzle and CD nozzle and a straight ejector were designed and simulated in 2-D. Meanwhile, the ejector position effect on the ejection performance of PDE based on the nozzle-ejector combinational structure was also considered. Several benefit conclusions were as follows by the numerical study.

- Nozzle type and ejector axial position both had important influence on the propulsion performance of a PDE.
- For a PDE with a convergent nozzle-ejector combinational structure, the best propulsive performance was obtained at the ejector position of  $x/d = +1$  among the three ejector positions. For a PDE with a CD nozzle-ejector combinational structure, the best propulsive performance was obtained at the ejector position of  $x/d = -1$ . For a PDE with a straight nozzle-ejector combinational structure, the best propulsive performance was obtained at the ejector position of  $x/d = 0$ .

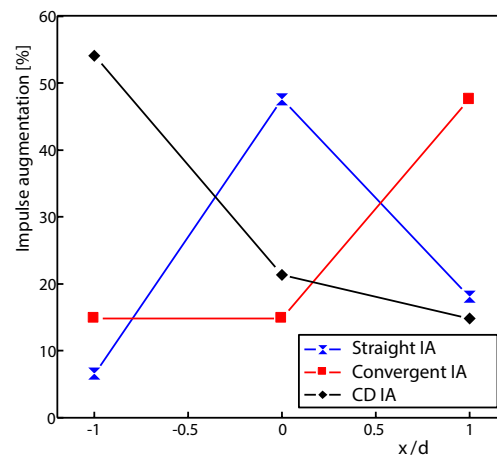


Figure 10. The experiment results of different nozzle-ejector combinations

- When the PDE was installed with the convergent nozzle-ejector combinational structure, the maximum impulse augmentation and the second largest ejection ratio was obtained at the ejector position of  $x/d = +1$ , which was indicated the best ejection performance.

### Acknowledgment

This work was financially supported by the National Natural Science Foundation of China through Grant No. (91741116, 51306153), the Natural Science Foundation of Shaanxi Province of China through Grant No. (2017JZ011), Science and Technology Foundation for Selected Overseas Scholar of Shaanxi Province of China (Grant No. 2017009), and the Fundamental Research Funds for the Central Universities (Grant No. 3102017jg02009).

### Nomenclature

$d$	– inner diameter of the detonation tube	$t$	– time, [s]
$F$	– force, [N]	$x$	– distance between the ejector inlet and the nozzle outlet
$I$	– impulse of the PDE with a convergent or convergent-divergent nozzle without ejector	<i>Greek symbols</i>	
$I_{ejector}$	– impulse of the PDE with a nozzle-ejector	$\lambda$	– the size of fuel cell
$I_{straight}$	– impulse of the PDE with the straight nozzle without ejector	<i>Acronyms</i>	
$IA$	– impulse augmentation based on a convergent or convergent-divergent nozzle	CD	– convergent-divergent
$IA_{straight}$	– impulse augmentation based on the straight nozzle	CEA	– chemical equilibrium and applications
$L$	– length of the detonation tube	CJ	– Chapman-Jouguet
$L_{DDT}$	– the DDT distance	DDT	– deflagration to detonation transition
$t$	– detonation initiation time	ER	– ejection ratio
		IA	– impulse augmentation
		PDE	– pulse detonation engine
		PISO	– pressure implicit with splitting of operators

### Reference

- [1] Fan, W., *et al.*, Experimental Investigation on Two-Phase Pulse Detonation Engine, *Combustion and Flame*, 133 (2003), 4, pp. 441-450
- [2] Kawane, K., *et al.*, The Influence of Heat Transfer and Friction on the Impulse of a Detonation Tube, *Combustion and Flame*, 158 (2011), 10, pp. 2023-2036
- [3] Yan, C., *et al.*, Exploratory Research of New Concept Pulse Detonation Engine, *Progress in Natural Science*, 12 (2002), 10, pp. 1021-1025
- [4] Yan, C., *et al.*, Research and Development of Pulse Detonation Engine, *Journal of Aerospace Power*, 16 (2001), 3, pp. 212-217
- [5] Fan, W., *et al.*, Recent Developments of New Concept Pulse Detonation Engine, *Aircraft design*, 23 (2003), 2, pp. 55-61
- [6] Zhang, Q., *et al.*, Conceptual Design of Multi-Cycle Pulse Detonation Engine, *Propulsion Technology*, 24 (2003), 6, pp. 500-504
- [7] Landry, K., *et al.*, Effect of Operating Frequency on PDE Driven Ejector Thrust Performance, *Proceedings*, 41<sup>st</sup> AIAA/ASME/SAE/ASEE Joint Propulsion Conference & Exhibit, Tucson, Ariz., USA, 2005
- [8] Cantein, G., *et al.*, Experimental and Numerical Investigations on PDE Performance Augmentation by Means of an Ejector, *Shock Waves*, 15 (2006), 2, pp.103-112
- [9] Wilson, J., A Simple Model of Pulsed Ejector Thrust Augmentation, NASA CR 2003-212541, Hanover, Md, USA, 2003
- [10] Gao, Z., *et al.*, Effect of the Axial Position of Tapered Ejector on the Pulse Detonation Rocket Engine Performance, *Propulsion Technology*, 33 (2012), 5, pp. 826-830
- [11] Wilkinson, D. R., *et al.*, Analysis of an Ejector-Augmented Pulse Detonation Rocketed, *Proceedings*, 46<sup>th</sup> AIAA Aerospace Sciences Meeting and Exhibit, AIAA 2008-114, Reno, Nev., USA, 2008
- [12] Glaser, A. J., *et al.*, Experimental Study of Ejectors Driven by a Pulse Detonation Engine, *Proceedings*, AIAA Space Conference and Exposition, AIAA 2007-447, Long Beach, Cal., USA, 2007

- [13] Bravo, L. G., *et al.*, Experimental Study of Rounded Ejector Inlets for Pulse Detonation Engines, <http://forms.gradsch.psu.edu/diversity/sroppapers/2004/BravoLuis.pdf>, paper AIAA 04-14342
- [14] Choutapalli, I., *et al.*, Pulsed Jet: Ejector Characteristics, *Proceedings*, 44<sup>th</sup> AIAA Aerospace Sciences Meeting & Exhibit, Reno, Nev., USA, 2006
- [15] Opalski, A. B., Detonation Driven Ejector Exhaust Flow Characterization Using Planar DPIV, *Proceedings*, 41<sup>st</sup> AIAA/ASME/SAE/ASEE Joint Propulsion Conference & Exhibit, AIAA 2005-4379, Tucson, Ariz., USA, 2005
- [16] Kazuhiko, T., *et al.*, Improvement of a Propulsion Equipment with a Supersonic Nozzle for Single Pulse Detonation, *Open Journal of Fluid Dynamics*, 4 (2014), 5, pp. 447-453
- [17] Farahi, M. H., *et al.*, Measure Theoretical Approach for Optimal Shape Design of a Nozzle, *Journal of Applied Mathematics and Computing*, 2005, 17 (2005), 1, pp. 315-328
- [18] Peng, C., *et al.*, Experimental Study of an Air-Breathing Pulse Detonation Engine Ejector, *Experimental Thermal and Fluid Science*, 35 (2011), 6, pp. 971-977
- [19] He, L., *et al.*, Analysis of Ejector Forms Effect of Pulse Detonation Engine Performance, *Aerodynamics Journal*, 27 (2009), 6, pp. 718-722
- [20] He, L., *et al.*, Effect of Ejector Throat Area Ratio on Pulse Detonation Engine Performance, *Aeroengine*, 37 (2011), 2, pp. 1-4
- [21] Li, M. C., Numerical Simulation and Verification of Pulse Detonation Engine Ejector Mode, *Journal of Aerospace Power*, 20 (2005), 4, pp.645-650
- [22] Qin, Y., *et al.*, Performance of Ring Pulse Detonation Engine Ejector, *Journal of Aerospace Power*, 26 (2011), 1, pp. 35-41
- [23] Huang, X., *et al.*, Experimental Study on Thrust Augmentation of Ejector Driven by Pulse Detonation Engine, *Journal of Northwestern Polytechnical University*, 31 (2013), 2, pp. 55-59
- [24] Wang, Y., *et al.*, Experimental Investigation on Initiation in Main Detonation Chamber at Ejector Mode of a PDRE, *Journal of Propulsion Technology*, 34 (2013), 8, pp. 1148-1152
- [25] Guo, K., *et al.*, Computational Study on Unsteady Flows in a Diverging Ejector for Pulse Detonation Engine, *Journal of Propulsion Technology*, 36 (2015), 12, pp. 1782-1787
- [26] Wang, Z., *et al.*, Investigation of Hot Jet Effect on Detonation Initiation Characteristics, *Combustion Science and Technology*, 189 (2017), 3, pp. 498-519